ACS OMEGA

http://pubs.acs.org/journal/acsodf

Article

Adsorptive Desulfurization of Condensate Contains Aromatic Compounds Using a Commercial Molecular Sieve

Amir Behbahani Nezhad, Farzad Bastan, Ahmad Panjehshahin,* and Mahdi Zamani

Cite This: *ACS Omega* 2023, 8, 10365−10372

Read Online

ACCESS | Metrics & More | Article Recommendations

ABSTRACT: This study is undertaken to evaluate the potential of a commercial molecular sieve to remove diverse sulfur compounds from condensate with high aromatic on an industrial scale. For the first part of this study, the adsorbent is characterized in detail using inductively coupled plasma optical emission spectroscopy, X-ray diffraction, field-emission scanning electron microscopy, and Brunauer−Emmett−Teller analysis. For the second part, dynamic breakthrough experiments on an industrial scale are performed to assess the dynamic adsorption performance of a commercial molecular sieve. Dynamic experiments show that the adsorbent effectively removes the sulfur compound from condensate that has approximately 900 ppmw S. In more detail, this commercial molecular sieve selectively desulfurizes condensate to about 12 ppmw S, and this is achieved when the concentration of non-sulfur aromatic is greater than 15 times higher than the total sulfur. As regeneration is a crucial part of the continuous adsorption−regeneration cycling process, the final part of this study is focused on finding a desorption method to avoid a sulfur concentration peak in tail gas.

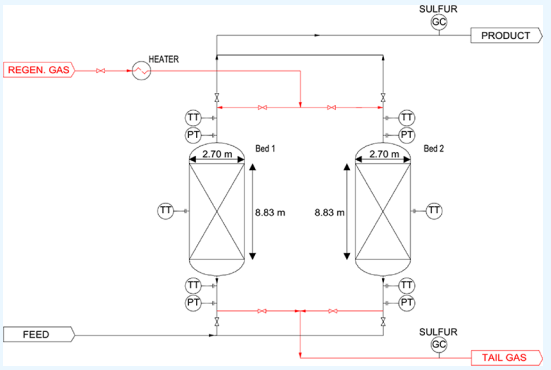

1. INTRODUCTION

Sulfur compounds, particularly sulfur oxides (SOx), cause various environmental hazards and industrial damage. In the petroleum industries, sulfur compounds cause pipeline corrosion, jeopardizing distribution networks, reducing the oil and gas quality, and poisoning or deactivating the downstream catalysts.[1−3] Thus, there has been a high demand for producing sulfur-free petroleum fuels and intermediate products recently.[4] Moreover, stringent environmental rules and regulations have been imposed on the allowable sulfur concentration of transportation fuels to minimize the adverse effects of sulfur emissions into the air.[1,5] To remove sulfur contained in petroleum fractions, numerous methods such as hydrodesulfurization, pervaporation, adsorption, biodesulfurization, extraction, and oxidation have been used.[6,7] Among these methods, hydrodesulfurization (HDS) has been the most widely used technology for removing sulfur compounds in refineries in the past few decades.[8,9] HDS is a catalytic process that involves a reaction with hydrogen and converts organosulfur compounds to H_2S and sulfur-free compounds. However, the HDS method highly depends on the structure of the sulfur compound, which has lower efficiency in aromatic sulfur structures such as thiophenes and also reduces the octane number of fuels by the side reactions.[10−12] Moreover, the HDS process requires high-cost external hydrogen, high pressure (50−100 bar), high temperature (300−400 °C), and suitable catalysts; therefore, the operation cost in this method is relatively high.[7] To overcome these drawbacks, non-HDS technologies, which should have lower energy consumption and be more efficient, have been explored to replace the current HDS technology. Adsorptive desulfurization, which has a low-energy demand (mild temperature and pressure), easy operation, relatively cheap adsorbent, and ultra-deep sulfur removal (<10 ppmw), is one of the most alternative techniques for sulfur removal in the refineries.[13−16]

Adsorption is defined as a process of moving an ion or molecule (adsorbate) from the bulk fluid phase and attached to the surface of a solid particle (adsorbent) through physical interactions or chemical bonds.[17,18] In adsorptive desulfurization, sulfur compounds from gaseous or liquid bulk interact with and become retained on the surface of the adsorbent. The selection of an effective adsorbent is a critical parameter in this process, and a wide variety of adsorbents based on zeolite, metal oxide, mesoporous material, activated carbon, modified carbon, and metal−organic frameworks have been used.[19,20] These materials can have amorphous (activated carbons) and/

Received: December 19, 2022
Accepted: February 23, 2023
Published: March 7, 2023

or crystalline structures (zeolites) at both the nano- and macroscale.[18] The main requirements for efficient desulfurization are high surface area per unit volume, stable structure, low cost, high regeneration capability, and selectivity.[21,22] Molecular sieves or synthetic zeolites not only have regenerability, stable structure, and a high number of mesopores but also have high selectivity and affinity toward sulfur compounds; therefore, they have been known as commercial adsorbents in the desulfurization process.[23]

The main difference between the types of synthetic zeolites is their structure and silicon−aluminum ratio (Si/Al). The polarity of zeolites can be changed by the Si/Al ratio. Zeolites with lower Si/Al ratios tend to adsorb polar substances more, whereas a higher Si/Al ratio leads to adsorbing nonpolar substances and has stable structures at higher temperatures.[24,25] The Si/Al ratio 1−1.5 is defined as zeolite X and Si/Al more than 1.5 is defined as zeolite Y.[26] In addition, zeolites can be modified with various metal ions to enhance adsorption capacity and selectivity toward target molecules.[18] Huang et al.[27] used copper ammonia solution as the ion-exchange media to enhance the adsorption capacity for both NaY (Si/Al = 2.3) and NaX (Si/Al = 1.23) zeolites. They found that the adsorbed amount of benzothiophene (BT) is enhanced and the Cu(*I*)X zeolite has a higher adsorption capacity compared to Cu(*I*)Y. Velu et al.[28] used NiY, CuY, ZnY, CeY, PdY, and HY zeolites to remove sulfur from JP-8 jet fuel with high sulfur content (736 ppm) and reported that zeolite Y exchanged with Pd and Ce had a higher sulfur adsorption capacity. Moreover, Sotelo et al.[29] investigated the influence of exchanged cations of Cs^+, K^+, and Na^+ at different Si/Al ratios (1.07−2.85) on the adsorption capacity and affinity of BT dissolved in cyclohexane. Their experiments indicate that in equilibrium experiments, decreasing the Si/Al and the electronegativity of the exchange cations increased the basicity and affinity toward the adsorbents, while in dynamic experiments, basicity reduced the adsorption capacity. They conclude that the best performance in desulphurization could be reached by medium basicity. The presence of aromatic thiophenes and their derivative compounds decreased the adsorptive desulfurization performance as their structure and adsorption energy are similar to aromatic hydrocarbons. Yoosuk et al.[30] compared the effects of aromatic and nitrogen compounds in adsorptive desulfurization over NaY, NiY, LaY, and NiCeY zeolites in a fixed bed. The results showed that aromatic and nitrogen compounds decreased the sulfur adsorption capacity, while nitrogen compounds have more adverse effects. Yang et al.[31] investigated the adsorption of thiophene on transportation fuels with benzene compounds by using Cu^+ and Ag^+ zeolite Y. The results implied that the Ag^+ and Cu^+ zeolites preferentially adsorbed thiophene over benzene and Cu^+ made a stronger bond with thiophene than Ag^+, and the same trend was reported by Oliveira et al.[32] They studied the selectivity of zeolites with different transition metals (Ag, Zn, and Ni) between toluene and thiophene. As a result, selectivity toward thiophene was enhanced by transition metal ion-exchanged Y zeolites. Additionally, the zeolite containing silver (AgY) has the highest capacity among Ag, Zn, and Ni for the adsorption of thiophene. Mohammed et al.[33] investigated the desulfurization of heavy naphtha (600 ppm sulfur concentration) by combining oxidation with iron-promoted activated carbon or Cu^{2+}-promoted zeolite 13X in batch experiments. The outcomes show that combining an oxidation agent with an adsorbent could effectively remove the initial sulfur content of heavy naphtha.

A wide range of adsorbents have already been studied to find effective and efficient adsorbents for removing sulfur compounds from fuels. However, most reports on adsorptive desulfurization in the literature and patents were done in batch experiments.[34,35] Despite numerous research on adsorptive desulfurization, there is not currently adequate data on the industrial scale for the adsorption desulfurization of heavy hydrocarbons, and most studies are dedicated to batch experiments.

This study aims to examine the adsorption performance of a commercial molecular sieve on an industrial scale in the continuous adsorption−regeneration cycling process. The distinctive properties of the used hydrocarbon feed are the high sulfur content and aromatic compounds. The sulfur content in the feed is approximately 900 ppmw, which is a relatively high sulfur range. Therefore, deep desulfurization of this feed is a challenging issue. Moreover, aromatic compounds, due to the competitive adsorption with sulfur compounds, have a strong negative impact on adsorptive desulfurization. The adsorption performance is evaluated under dynamic conditions and plotting dynamic breakthrough curves in multiple adsorption−regeneration cycles. In addition, during the regeneration stage, releasing a high amount of sulfur from the molecular sieve into the purge gas increases the sulfur content to higher than acceptable limits; therefore, a reliable solution is found to avoid the sulfur peak during the regeneration of beds.

2. EXPERIMENTAL SECTION

2.1. Material. The adsorbent used in this study is a spherical molecular sieve with a diameter of 1.6−2.5 mm and characterized in detail by utilizing inductively coupled plasma optical emission spectroscopy (ICP-OES), X-ray diffraction (XRD), field-emission scanning electron microscopy (FE-SEM), and Brunauer−Emmett−Teller (BET) analysis. The condensate with high sulfur and aromatic compounds is used to investigate the performance of molecular sieves in the desulfurization process. The composition of condensate is summarized in Table 1.

2.2. Industrial Plant. Each adsorption process is followed by a regeneration stage in successive cycles. Therefore, two or more adsorption columns are used to perform the process continuously. In the industrial plant, which is discussed in this

Table 1. Feed (Condensate) Composition

component	unit	feed
paraffins	% mol	36.400
I-paraffins		55.417
olefins		0.059
naphthenes		6.648
aromatic		1.354
oxygenates		<0.010
total C13+		0.015
mercaptans	ppmw	1711
H_2S		3
thiophene		58
RSR		18
RSSR		156
total sulfur		899

https://doi.org/10.1021/acsomega.2c08051
ACS Omega 2023, 8, 10365−10372

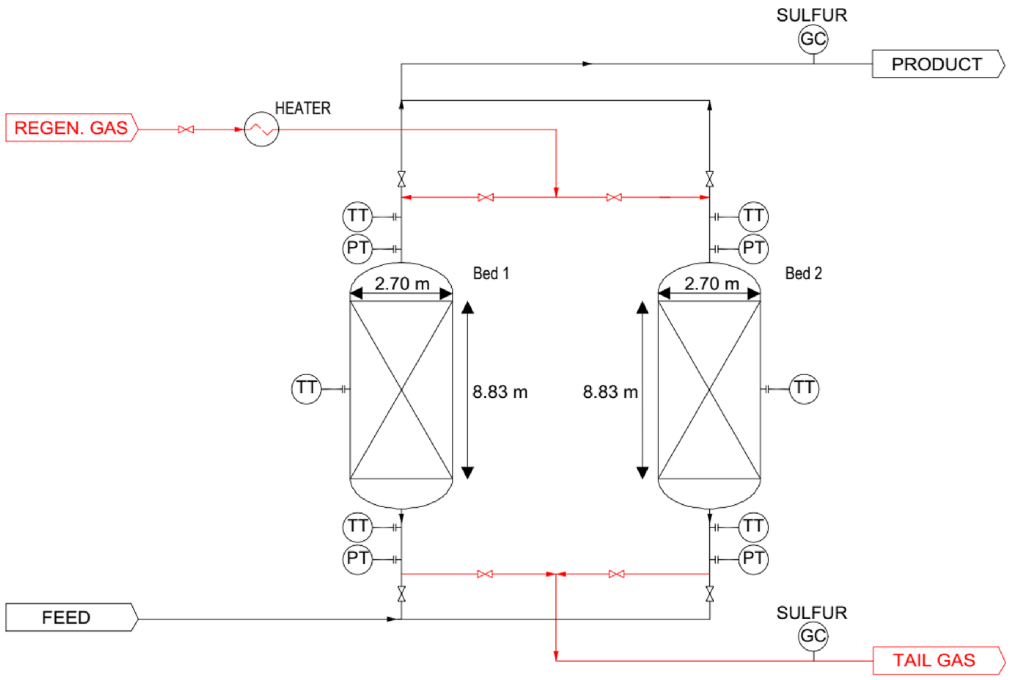

Figure 1. Schematic diagram of the adsorption desulfurization process (TT, temperature transmitter; PT, pressure transmitter; GC, gas chromatography).

article, the desulfurization process is carried out in two identical parallel beds (one bed under adsorption + one bed under regeneration). A schematic diagram of the beds and their auxiliary equipment is shown in Figure 1. The internal diameter of each bed is 2.70 m, and 8.83 m of the bed is filled with a molecular sieve. In each bed, approximately 33,000 kg of the molecular sieve is used to fill the beds. In more detail, a 15 cm layer of inert ceramic balls is loaded above and under the molecular sieve layer to distribute flow through the molecular sieve and prevent them from passing through the beds. Two floating screens of approximately 20 mesh stainless steel are installed on the top and bottom of beds to prevent particles from passing through the screen. In the following, the stages of adsorption and regeneration are described in detail.

2.2.1. Adsorption Stage. In this stage, sulfur compounds are separated from the condensate with a flow rate of 27,000 kg/h in the upward direction. The condensate at the upstream of the bed has a temperature of 110 °C, and to increase the adsorption efficiency, it is subcooled to 48.0 °C at 2.0 barg. In each bed, the pressure drop across the bed is approximately 0.4 barg, and the product is routed to the storage tank. The sulfur content in the product is continuously monitored by online gas chromatography (GC). If the sulfur content in the products increases more than the acceptable limit, the bed is switched to the regeneration mode.

2.2.2. Regeneration Stage. Adsorbed compounds must be removed from the adsorbent to restore the adsorption capacity for reuse in the next adsorption cycle. Therefore, the temperature swing adsorption (TSA) process is applied to release sufficient quantities of the sulfur components from the molecular sieve. The TSA process is based on regenerating the adsorbent bed at a temperature higher than used during adsorption. In this process, the fuel gas (mainly methane) with a flow rate of 9500 kg/h is passed through a heater, and a constant heating rate is used to increase the temperature of the fuel gas from 48 to 285 °C via a ramp. Hot fuel gas passes through the bed in counterflow (flow direction from top to bottom) and gradually heated the adsorbents. The adsorbed sulfur is released from the adsorbent surface into the fuel gas and collected in the tail gas. The sulfur concentration in tail gas is continuously measured and the regeneration step is completed when the sulfur content in tail gas is minimized. The industrial conditions of the adsorption and regeneration stage are summarized in Table 2.

Table 2. Industrial Conditions of the Adsorption and Regeneration Stage

adsorption stage	
temperature, °C	48.0
pressure, barg	2.0
flow rate, kg/h	27,000.0
duration, min	~3200.0
regeneration stage	
temperature, °C	285.0
pressure, barg	27.5
flow rate, kg/h	9500.0
duration, min	~840.0

3. RESULTS AND DISCUSSION

3.1. Characterization of Adsorbents. Characterization experiments, including ICP-OES, XRD, FE-SEM, and BET analysis, are conducted to determine the properties of the molecular sieve. The physical and chemical properties of adsorbents are essential to understand the adsorbent mechanism of the adhesion of sulfur compounds on the molecular sieve surface. ICP-OES analysis is employed to determine the chemical compositions of the adsorbent accurately using an Agilent 5800 ICP-OES instrument[36] (Table 3). As it was discussed, the silicon−aluminum ratio (Si/Al) has a crucial factor in the adsorption efficiency and is

https://doi.org/10.1021/acsomega.2c08051
ACS Omega 2023, 8, 10365−10372

Table 3. Chemical Composition of the Commercial Molecular Sieve Determined by ICP-OES Analysis

element	wt %
Mg	1.240
Si	9.720
Al	11.700
Cr	0.010
Mn	0.016
Pb	0.007
Ca	0.210
P	0.190
B	0.790
Fe	0.750
Na	10.100
Ti	0.021

calculated with the balance assumed to be oxygen. Therefore, the sample contained 100−1.24−9.72−11.7−0.01−0.016−0.007−0.21−0.19−0.79−0.75−10.1−0.021 = 65.246 wt % O. Thus, the Si/Al molar ratio is 0.8, which indicates a typical X zeolite type with 10.1 wt % sodium (Na). In addition, the traces of Mg, Ca, P, and also B could be found in the structure of the adsorbent.

The morphology of the molecular sieve is obtained by FE-SEM (Mira3-Tescan-XMU), and the representative images are presented in Figure 2. The micrographs' magnification of the adsorbent in the range of 5000−100,000 displays the shape and size of the adsorbent. These images specify that the molecular sieve has a crystalline structure and no noticeable amount of amorphous phases could be found. The images reveal that the adsorbent mainly consists of spherical particles with an average crystal size of 2.4 μm.

To confirm the crystallinity of the molecular sieve, the XRD is employed using a STOE-IPDS 2T diffractometer, and the results are analyzed by X'Pert HighScore Plus software. The obtained XRD pattern of the adsorbent ranging from 4 to 70° at 2θ is shown in Figure 3. The crystal structure of the material is assessed by the intensity, and the peak intensity reflects the crystallinity framework of them.[37] As can be seen, the main diffraction peaks of the molecular sieve around 2θ of 7, 12, 24, 26, 27, 30, 34, 41, 47, 52, 54, 58, 66, and 69° are distinguishable, and these sharp peaks reveal the presence of a highly crystalline structure.

Moreover, nitrogen adsorption isotherms at 77 K are employed to calculate the BET surface area, and the pore size distribution is determined by the Barrett−Joyner−Halenda (BJH) method. Figure 4a presents the N_2 adsorption−desorption for a commercial molecular sieve. According to the IUPAC classification,[38] a molecular sieve exhibits a typical type II isotherm with unrestricted mono−multilayer adsorption. In this form of isotherms, the adsorption is rising continuously, even though the pressure ratio is close to unity. From the pore size distribution of the BJH method (Figure 4b), the molecular sieve has a mesopore structure and bimodal pore size distribution that extend to macroporosity. The pore size distribution is in the range of 2.2 to 110 nm, which has two main peaks at 2.2 and 36.3 nm. A detailed summary of the textural parameters of the molecular sieve is represented in Table 4.

3.2. Breakthrough. To assess the sulfur adsorption capacity of the adsorbent, the total sulfur at the outlet of the bed is continuously measured. As a result, a dynamic breakthrough curve in multi-cycle adsorption and desorption is evaluated. The breakthrough curve analysis helps to understand the performance of an adsorption bed. The breakthrough time and the shape of the breakthrough curve show the efficiency of the bed in the adsorption-based separation process. In this article, the breakthrough test is carried out at 48 °C, 2.0 barg with a flow rate of 27,000 kg/h of condensate in the upward direction. Before the breakthrough experiment, the bed is heated by hot fuel gas at 285 °C and 27.5 barg for 10 h to remove any residuals that may have been presented on the surface of the molecular sieve. Subsequently, the bed is cooled down to reach 60 °C and depressurized to the ambient pressure. As it is explained in the process description, an online GC is installed at the product stream to record the sulfur content of the condensate (C) at the outlet of the bed. The initial concentration of sulfur (C_0) in the inlet of the bed is measured at regular intervals, and the breakthrough curve is constructed by plotting C/C_0 versus time (min). The sulfur component concentration in the condensate is 1946 ppmw (899 ppmw sulfur basis), and the initial concentration of sulfur at regular sampling remained almost steady. The dynamic breakthrough curve for a single adsorption process is presented in Figure 5. As can be observed, the adsorbent has a remarkable selectivity toward the sulfur compound and the sulfur content after the bed is less than 12 ppmw for approximately 1100 min. In an industrial plant, to match the commercial specification for production, adsorption capacity (at saturation) could not be measured as the bed should be switched to the regeneration mode when the C/C_0 ratio reaches approximately 0.1. The desulfurization efficiency (R) for the bed is calculated by the following equation:[33]

$$R\% = \frac{C_0 - C_{out}}{C_0} \quad (1)$$

The initial efficiency of the bed is 100%, and the bed is capable of removing the total sulfur content of condensate. After 1100 and 3200 min, the efficiency drops to 99.3 and 91.1%, respectively. Achieving high efficiency after 3200 min implies a high adsorption capacity of the molecular sieve.

Solvent−adsorbate interactions play an important role in the adsorptive desulfurization of condensate. As was discussed, thiophene and benzene have a similar structure; therefore, they will compete against the adsorbent for interaction. The condensate at the outlet of the bed is sampled, and the composition of sulfur compounds is measured (Table 5). It is obvious that the aromatic compounds at the outlet of the bed decreased from 1.354 to 0.066 mol % and the aromatic compounds are adsorbed significantly. Despite the amount of aromatic adsorption, the molecular sieve still has a high capacity toward sulfur compounds and could decrease 900 ppmw sulfur compound to 12 ppmw.

3.3. Effect of Multi-Cycle Adsorption−Desorption. The regenerability of the molecular sieve is one of the critical factors for the applicability of the adsorbent in industrial desulfurization. The aromatic adsorption could affect the regeneration of the adsorbent. If the aromatic compounds are not released in the regeneration stage, the working capacity of the adsorbent is decreased, so the adsorption time will be reduced either. To determine the influence of aromatic adsorption on continuous adsorption, the multi-cycle capability of the adsorbent is employed by regenerating the saturated adsorbent with fuel gas at elevated temperatures and

https://doi.org/10.1021/acsomega.2c08051
ACS Omega 2023, 8, 10365−10372

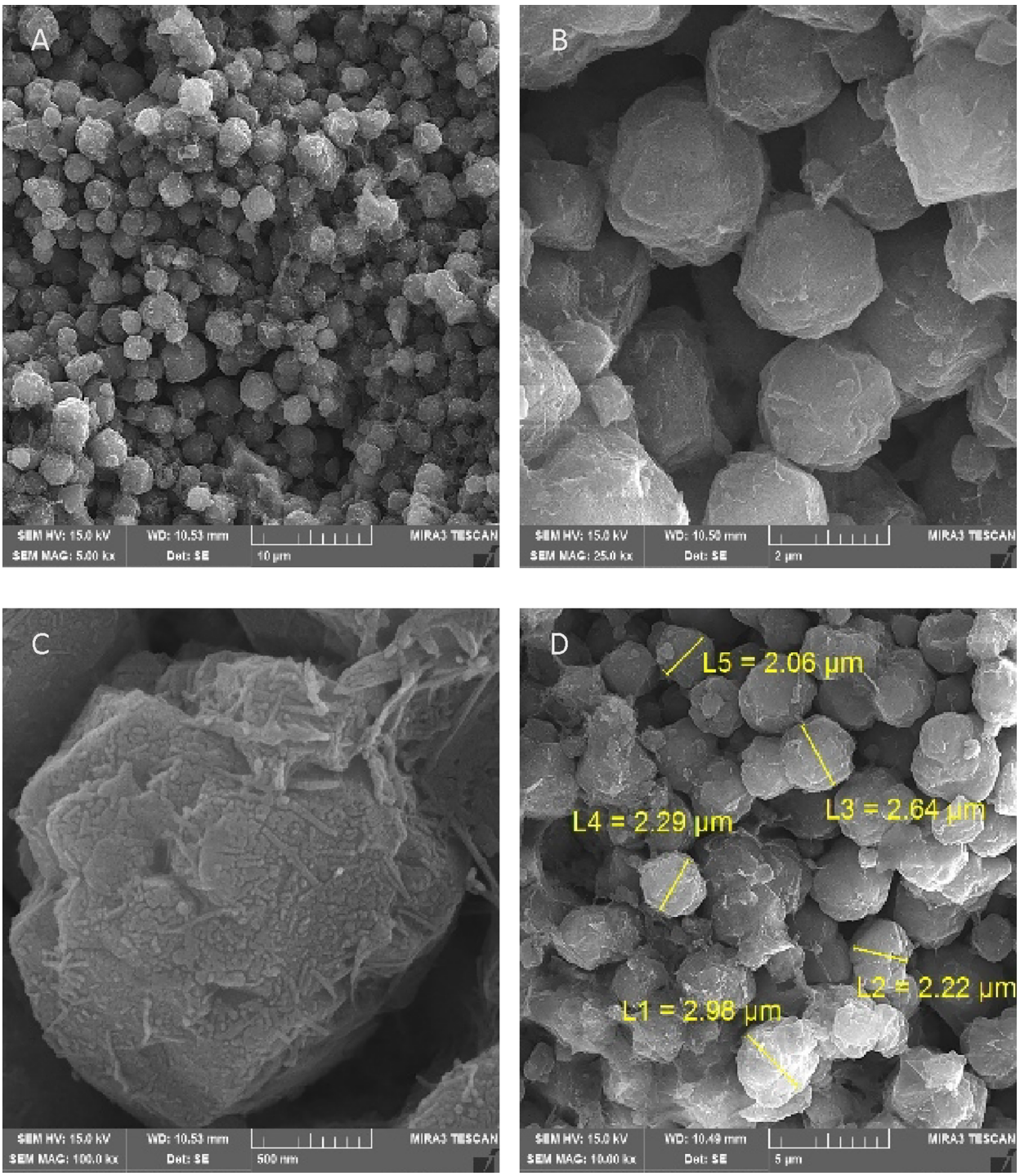

Figure 2. SEM images of the molecular sieve at different magnifications: (a) 5 KX, (b) 25 KX, (c) 100 KX, and (d) 10 KX.

dynamic breakthrough is examined through three cycles of adsorption−regeneration. After each adsorption stage, the saturated bed is heated by fuel gas at a temperature of 285 °C for 10 h, and then the bed is cooled to reach 60 °C. To employ a TSA system, the regeneration stage should be shorter or at most equal to the adsorption stage duration. In the regeneration process, the sulfur concentration (C) at the tail gas is measured continuously and normalized by the initial concentration of sulfur (C_0) in the condensate. As it is shown in Figure 6, despite the early adsorption of aromatic compounds, the breakthrough performance is consistent for multiple cycles. The regenerated adsorbent recovered as the total adsorption time did not decrease after returning from each regeneration stage.

3.4. Avoiding Sulfur Peak. During the regeneration stage, the large peak concentration of sulfur is unavoidable.[39] The sulfur peak in tail gas makes it out of acceptable specification and could not be used in downstream. In more detail, tail gas in downstream of the plant is mixed with export gas. Therefore, the high sulfur content in tail gas could increase the total sulfur content in export gas. As can be seen from Figure 7, during the bed regeneration by increasing the temperature from 48 to 285

https://doi.org/10.1021/acsomega.2c08051
ACS Omega 2023, 8, 10365−10372

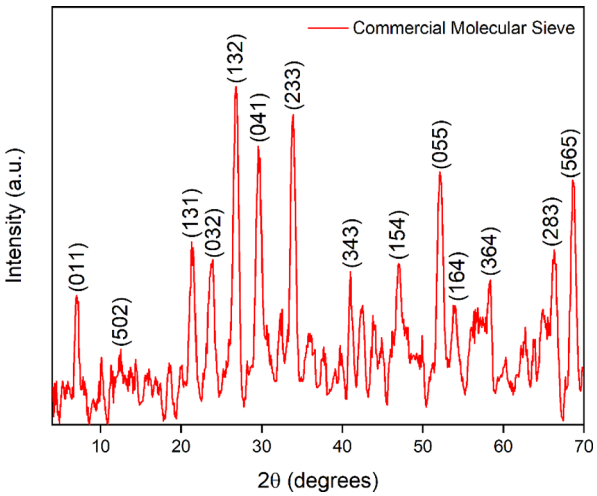

Figure 3. XRD pattern of the molecular sieve.

°C, the sulfur peak concentration is up to five times higher than the initial sulfur content in the feed. To avoid the sulfur peak in tail gas, the temperature ramp is changed from a single temperature ramp-up to two temperature ramp-ups (first ramp from 48 to 160 °C and second ramp from 160 to 285 °C). As a result, in the two temperature ramp-ups, the sulfur peak decreased significantly and stayed below two times. The main reason is that when the bed temperature is increased in one step and reaches 285 °C, the light and heavy sulfurs are removed from the adsorbent nearly at the same time and entered into the tail gas. Meanwhile, during the first step of the two temperature ramps, a lower temperature allows the light sulfur compounds to release from the bed. Therefore, in the second step, less sulfur remained in the bed, and as a result, a lower sulfur peak occurs at the higher temperature.

4. CONCLUSIONS

In this work, the dynamic adsorption performance of a commercial molecular sieve for desulfurization of condensate in the co-presence of aromatic compounds on an industrial scale is evaluated. For better evaluation, the commercial molecular sieve is characterized by ICP-OES, XRD, FE-SEM, and BET analysis. The results show that the Si/Al ratio of the adsorbent is 0.8 and contains 10.1 wt % sodium, which is an X zeolite type (NaX). In addition, the morphology of the adsorbent is crystalline and mainly consists of spherical particles with an average crystal size of 2.4 μm. Moreover, the BET characterization results indicated that the adsorbent has a mesopore structure that extends to macroporosity and has a high surface area of 747 m^2/g. The adsorption desulfurization performance of the adsorbent is calculated by the dynamic breakthrough curve in multi-cycle adsorption−regeneration, which shows that the adsorbent is capable of removing sulfur compounds in the condensate from approximately 900 ppmw to less than 12 ppmw during nearly 1100

Table 4. Specific Surface Area and Pore Volume of the Commercial Molecular Sieve

textural parameters	value
BET surface area, $m^2\ g^{-1}$	747.63
pore volume, $cm^3\ g^{-1}$	0.14
average pore size, nm	2.26
external surface area, $m^2\ g^{-1}$	67.97
micropore area, $m^2\ g^{-1}$	679.66
micropore volume, $cm^3\ g^{-1}$	0.32

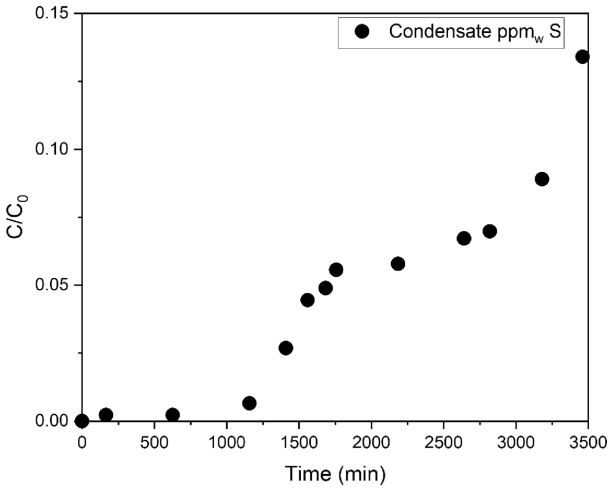

Figure 5. Breakthrough curve of the commercial molecular sieve for desulfurization of condensate.

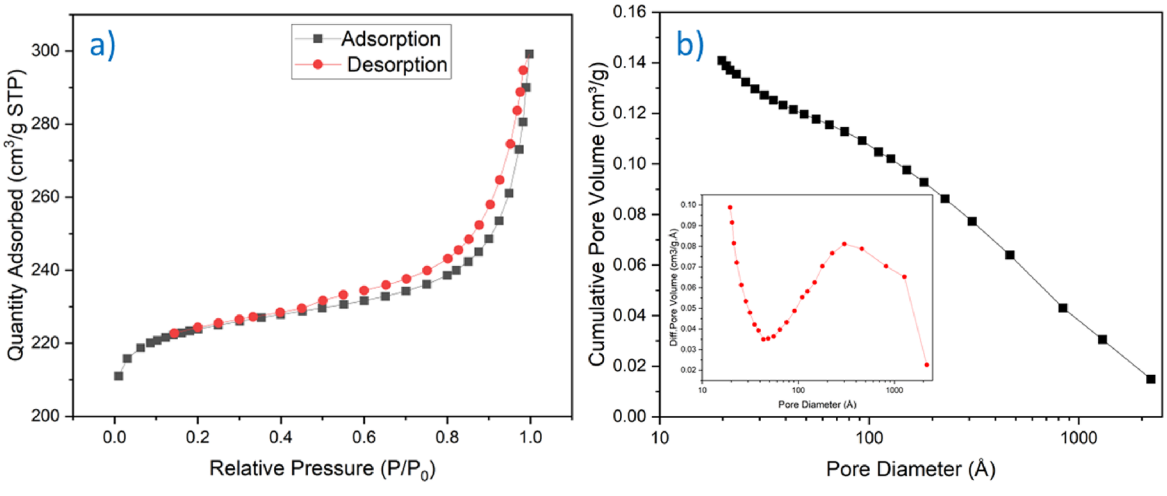

Figure 4. (a) N2 adsorption−desorption isotherm and (b) pore size distributions calculated by the BJH method.

https://doi.org/10.1021/acsomega.2c08051
ACS Omega 2023, 8, 10365−10372

Table 5. Condensate Composition after the Treatment

component	unit	product
paraffins	% mol	36.667
I-paraffins		56.288
olefins		0.044
naphthenes		6.635
aromatic		0.066
oxygenates		0.173
total C13+		0.034
mercaptans	ppmw	11.2
H_2S		2.0
thiophene		<1.0
RSR		<1.0
RSSR		<1.0
total sulfur		12.0

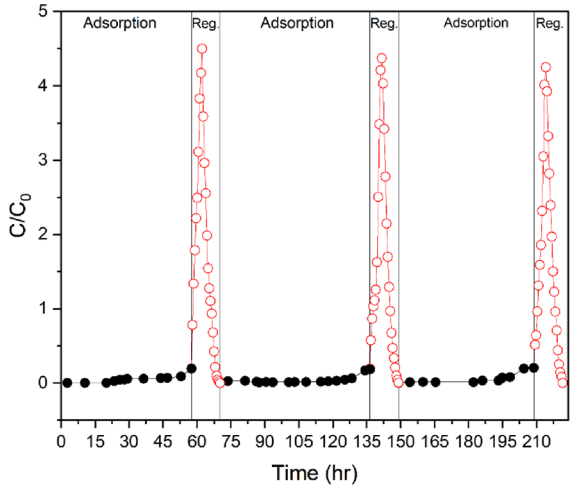

Figure 6. Breakthrough performance for three cycles of adsorption−desorption.

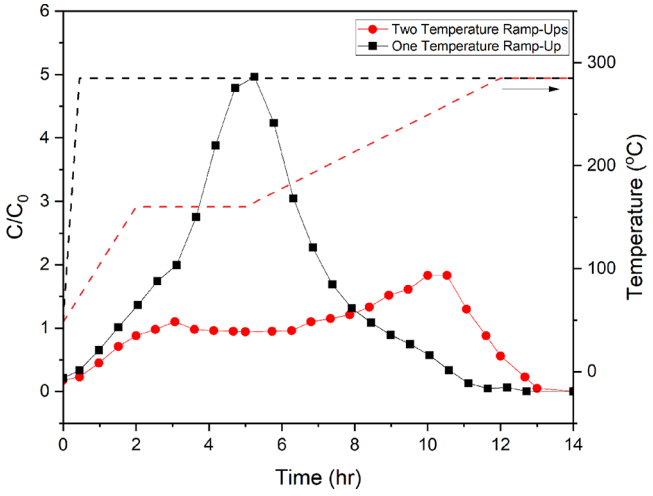

Figure 7. Comparison of the sulfur peak concentration at two different temperature ramp-ups.

min. Based on the acceptable sulfur content limit (C/C_0 equal to 0.1), the bed could stay in the adsorption stage for about 3200 min, which indicates its high adsorption capacity. Despite the early adsorption of aromatic, the molecular sieve still has a high capacity toward sulfur compounds and it is able to remove sulfur compounds for long periods. The adsorption of aromatic compounds does not affect the regeneration stage as the adsorption time is not decreased at each cycle and the bed could remove adsorbate from the molecular sieve in the regeneration stage. Furthermore, we tried to find an applicable solution to avoid sulfur peak concentration during the regeneration stage. By changing the temperature curve from a single temperature ramp to two temperature ramps, the sulfur peak on tail gas decreases substantially to 40% of the initial peak. It is worth mentioning that the adsorption capacity at saturation could not be measured in an industrial plant. The focus of future work should therefore increasingly be on investigating the capacity of the adsorbent in various conditions to deeply understand the applicability of the adsorbent on other feeds and conditions.

AUTHOR INFORMATION

Corresponding Author

Ahmad Panjehshahin − *Department of Chemical and Petroleum Engineering, Sharif University of Technology, Tehran 7571855177, Iran;* orcid.org/0000-0001-5339-8292; Email: ahmad.panjehshahin@alum.sharif.edu

Authors

Amir Behbahani Nezhad − *Department of Chemical and Petroleum Engineering, Tehran University, Tehran 11365-11155, Iran*

Farzad Bastan − *Department of Chemical and Petroleum Engineering, Sharif University of Technology, Tehran 7571855177, Iran*

Mahdi Zamani − *Department of Chemical and Petroleum Engineering, Tehran University, Tehran 11365-11155, Iran*

Complete contact information is available at: https://pubs.acs.org/10.1021/acsomega.2c08051

Notes

The authors declare no competing financial interest.

ACKNOWLEDGMENTS

The authors acknowledge Sharif University of Technology for its valuable support in this work and the research behind it.

REFERENCES

(1) Saleh, T. A. Carbon Nanotube-Incorporated Alumina as a Support for MoNi Catalysts for the Efficient Hydrodesulfurization of Thiophenes. *Chem. Eng. J.* **2021**, *404*, No. 126987.

(2) Strogen, B.; Bell, K.; Breunig, H.; Zilberman, D. Environmental, Public Health, and Safety Assessment of Fuel Pipelines and Other Freight Transportation Modes. *Appl. Energy* **2016**, *171*, 266−276.

(3) Mohebi, S.; Darvishi, A.; Hosseini, S.; Bolhasani, A.; Karamian, S.; Dehghani, O.; Khanbolouk, F. Investigation of the Effect of Presulphidation on Coke Deposition on 25Cr-35Ni Alloy during Ethane Steam Cracking. *Can. J. Chem. Eng.* **2022**, DOI: 10.1002/cjce.24638.

(4) Saha, B.; Vedachalam, S.; Dalai, A. K. Review on Recent Advances in Adsorptive Desulfurization. *Fuel Process. Technol.* **2021**, *214*, No. 106685.

(5) Saleh, T. A. Global Trends in Technologies and Nanomaterials for Removal of Sulfur Organic Compounds: Clean Energy and Green Environment. *J. Mol. Liq.* **2022**, No. 119340.

(6) Fihri, A.; Mahfouz, R.; Shahrani, A.; Taie, I.; Alabedi, G. Pervaporative Desulfurization of Gasoline: A Review. *Chem. Eng. Process* **2016**, *107*, 94−105.

(7) Saleh, T. A. Characterization, Determination and Elimination Technologies for Sulfur from Petroleum: Toward Cleaner Fuel and a Safe Environment. *Trends Environ. Anal. Chem.* **2020**, *25*, No. e00080.

(8) Saleh, T. A. Simultaneous Adsorptive Desulfurization of Diesel Fuel over Bimetallic Nanoparticles Loaded on Activated Carbon. *J. Cleaner Prod.* **2018**, *172*, 2123−2132.
(9) Al-Jamimi, H. A.; BinMakhashen, G. M.; Saleh, T. A. Multiobjectives Optimization in Petroleum Refinery Catalytic Desulfurization Using Machine Learning Approach. *Fuel* **2022**, *322*, No. 124088.
(10) Guo, Y.; Xie, W.; Li, H.; Li, J.; Hu, J.; Liu, H. Construction of Hydrophobic Channels on Cu (I)-MOF Surface to Improve Selective Adsorption Desulfurization Performance in Presence of Water. *Sep. Purif. Technol.* **2022**, *285*, No. 120287.
(11) Fox, B. R.; Brinich, B. L.; Male, J. L.; Hubbard, R. L.; Siddiqui, M. N.; Saleh, T. A.; Tyler, D. R. Enhanced Oxidative Desulfurization in a Film-Shear Reactor. *Fuel* **2015**, *156*, 142−147.
(12) Bian, H.; Zhang, H.; Li, D.; Duan, Z.; Zhang, H.; Zhang, S.; Xu, B. Insight into the Oxidative Desulfurization Mechanism of Aromatic Sulfur Compounds over Ti-MWW Zeolite: A Computational Study. *Microporous Mesoporous Mater.* **2020**, *294*, No. 109837.
(13) Saleh, T. A.; Sulaiman, K. O.; Al-Hammadi, S. A.; Dafalla, H.; Danmaliki, G. I. Adsorptive Desulfurization of Thiophene, Benzothiophene and Dibenzothiophene over Activated Carbon Manganese Oxide Nanocomposite: With Column System Evaluation. *J. Cleaner Prod.* **2017**, *154*, 401−412.
(14) Kim, J. H.; Ma, X.; Zhou, A.; Song, C. Ultra-Deep Desulfurization and Denitrogenation of Diesel Fuel by Selective Adsorption over Three Different Adsorbents: A Study on Adsorptive Selectivity and Mechanism. *Catal. Today* **2006**, *111*, 74−83.
(15) Danmaliki, G. I.; Saleh, T. A.; Shamsuddeen, A. A. Response Surface Methodology Optimization of Adsorptive Desulfurization on Nickel/Activated Carbon. *Chem. Eng. J.* **2017**, *313*, 993−1003.
(16) Zhou, T.; Wang, S.; Zhang, C.; Yao, Y.; Chen, Y.; Lu, S.; Liao, X. Preparation of Ti-MOFs for Efficient Adsorptive Desulfurization: Synthesis, Characterization, and Adsorption Mechanisms. *Fuel* **2023**, *339*, No. 127396.
(17) Dąbrowski, A. Adsorption—from Theory to Practice. *Adv. Colloid Interface Sci.* **2001**, *93*, 135−224.
(18) Georgiadis, A. G.; Charisiou, N. D.; Goula, M. A. Removal of Hydrogen Sulfide from Various Industrial Gases: A Review of the Most Promising Adsorbing Materials. *Catalysts* **2020**, *10*, 521.
(19) Lee, K. X.; Valla, J. A. Adsorptive Desulfurization of Liquid Hydrocarbons Using Zeolite-Based Sorbents: A Comprehensive Review. *React. Chem. Eng.* **2019**, *4*, 1357−1386.
(20) Saleh, T. A.; Danmaliki, G. I. Adsorptive Desulfurization of Dibenzothiophene from Fuels by Rubber Tyres-Derived Carbons: Kinetics and Isotherms Evaluation. *Process Saf. Environ. Prot.* **2016**, *102*, 9−19.
(21) Georgiadis, A. G.; Charisiou, N.; Yentekakis, I. V.; Goula, M. A. Hydrogen Sulfide (H2S) Removal via MOFs. *Materials* **2020**, *13*, 3640.
(22) Ullah, R.; Tuzen, M.; Ullah, S.; Haroon, M.; Khattak, R.; Saleh, T. A. Acidic Sites Enhanced Ultra-Deep Desulfurization Performance of Novel NiZnO-Based Mixed Oxides Mesoporous Adsorbents. *Surf. Interfaces* **2023**, *36*, No. 102566.
(23) Siakavelas, G. I.; Georgiadis, A. G.; Charisiou, N. D.; Yentekakis, I. V.; Goula, M. A. Cost-Effective Adsorption of Oxidative Coupling-Derived Ethylene Using a Molecular Sieve. *Chem. Eng. Technol.* **2021**, *44*, 2041−2048.
(24) Kristóf, T. Selective Removal of Hydrogen Sulphide from Industrial Gas Mixtures Using Zeolite NaA. *Hungarian J. Ind. Chem.* **2017**, *45*, 9−15.
(25) Georgiadis, A. G.; Charisiou, N. D.; Gaber, S.; Polychronopoulou, K.; Yentekakis, I. V.; Goula, M. A. Adsorption of Hydrogen Sulfide at Low Temperatures Using an Industrial Molecular Sieve: An Experimental and Theoretical Study. *ACS Omega* **2021**, *6*, 14774−14787.
(26) Kulprathipanja, S. *Zeolites in Industrial Separation and Catalysis*; John Wiley & Sons, 2010.
(27) Huang, E.; Xu, Y.; Ren, Y.; Zhang, P.; Zeng, Y. Cu (I)-Faujasite-Type Zeolites with Hierarchical Structure for Adsorption Desulfurization. *Microporous Mesoporous Mater.* **2023**, *348*, No. 112397.
(28) Velu, S.; Ma, X.; Song, C. *Zeolite-Based Adsorbents For Desulfurization Of Jet Fuel By Selective Adsorption*; Fuel Chemistry Division Preprints, 2002.
(29) Sotelo, J. L.; Uguina, M. A.; Águeda, V. I. Fixed Bed Adsorption of Benzothiophene over Zeolites with Faujasite Structure. *Adsorption* **2007**, *13*, 331−339.
(30) Yoosuk, B.; Silajan, A.; Prasassarakich, P. Deep Adsorptive Desulfurization over Ion-Exchanged Zeolites: Individual and Simultaneous Effect of Aromatic and Nitrogen Compounds. *J. Cleaner Prod.* **2020**, *248*, No. 119291.
(31) Yang, R. T.; Hernández-Maldonado, A. J.; Yang, F. H. Desulfurization of Transportation Fuels with Zeolites under Ambient Conditions. *Science* **2003**, *301*, 79−81.
(32) Oliveira, M. L. M.; Miranda, A. A. L.; Barbosa, C.; Cavalcante, C. L., Jr.; Azevedo, D. C. S.; Rodriguez-Castellon, E. Adsorption of Thiophene and Toluene on NaY Zeolites Exchanged with Ag (I), Ni (II) and Zn (II). *Fuel* **2009**, *88*, 1885−1892.
(33) Mohammed, M. M.; Alalwan, H. A.; Alminshid, A.; Hussein, S. A. M.; Mohammed, M. F. Desulfurization of Heavy Naphtha by Oxidation-Adsorption Process Using Iron-Promoted Activated Carbon and Cu+ 2-Promoted Zeolite 13X. *Catal. Commun.* **2022**, *169*, No. 106473.
(34) Saleh, T. A.; Danmaliki, G. I. Influence of Acidic and Basic Treatments of Activated Carbon Derived from Waste Rubber Tires on Adsorptive Desulfurization of Thiophenes. *J. Taiwan Inst. Chem. Eng.* **2016**, *60*, 460−468.
(35) Ma, X.; Sprague, M.; Song, C. Deep Desulfurization of Gasoline by Selective Adsorption over Nickel-Based Adsorbent for Fuel Cell Applications. *Ind. Eng. Chem. Res.* **2005**, *44*, 5768−5775.
(36) Jandaghian, M. H.; Maddah, Y.; Sepahi, A.; Hosseini, S.; Nikzinat, E.; Masoori, M.; Afzali, K.; Rashedi, R.; Houshmandmoayed, S. Chlorination of Mg (OEt) 2 with Halocarbons: A Promising Approach for Eliminating Chlorine-Containing Activators from Ziegler−Nattas' Recipes. *Ind. Eng. Chem. Res.* **2022**, *61*, 11708−11717.
(37) Jandaghian, M. H.; Maddah, Y.; Hosseini, S.; Eshaghzadeh, F.; Sepahi, A.; Nikzinat, E.; Masoori, M.; Bazgir, H.; Rashedi, R. Demystifying the Two-Sided Role of Inorganic Halides in the Structure and Performance of Ziegler−Natta Catalysts. *Mol. Syst. Des. Eng.* **2022**, *7*, 1722−1735.
(38) Thommes, M.; Kaneko, K.; Neimark, A. V.; Olivier, J. P.; Rodriguez-Reinoso, F.; Rouquerol, J.; Sing, K. S. W. Physisorption of Gases, with Special Reference to the Evaluation of Surface Area and Pore Size Distribution (IUPAC Technical Report). *Pure Appl. Chem.* **2015**, *87*, 1051−1069.
(39) Kidnay, A. J.; Parrish, W. R. *Fundamentals of Natural Gas Processing*; CRC press, 2006, DOI: 10.1201/9781420014044.

https://doi.org/10.1021/acsomega.2c08051
ACS Omega 2023, 8, 10365−10372